

Osteoconductivity and Growth Factor Production by MG63 Osteoblastic Cells on Bioglass-Coated Orthopedic Implants

Fei Tan,^{1,2,3} Mariam Naciri,^{1,2} Mohamed Al-Rubeai^{1,2}

¹School of Chemical and Bioprocess Engineering, University College Dublin, Belfield, Dublin 4, Ireland; telephone: 353-1-7161862; fax: 353-1-716-1177; e-mail: m.al-rubeai@ucd.ie

²Conway Institute of Biomolecular and Biomedical Research, University College Dublin, Belfield, Dublin, Ireland

³School of Medicine and Medical Science, University College Dublin, Belfield, Dublin, Ireland

Received 20 May 2010; revision received 2 September 2010; accepted 7 September 2010

Published online 24 September 2010 in Wiley Online Library (wileyonlinelibrary.com). DOI 10.1002/bit.22955

ABSTRACT: We have produced Bioglass coatings for Orthopedic implants by using a novel coating technique, CoBlast. The two resultant surfaces, designated BG and hydroxyapatite (HA)/BG, were compared with their HA counterpart, OsteoZip in terms of osteoblastic cell attachment, adhesion, proliferation, differentiation, and growth factor production. BG and HA/BG were demonstrated by goniometry to be more hydrophilic than OsteoZip. This corresponded to enhanced protein adsorption, cell attachment, and cell adhesion documented by both quantitative and qualitative assessments. BG and HA/BG surfaces had a significant initial release of Si and Ca ions, and this was consistent with elevated cell proliferation and basic fibroblast growth factor levels. However, OsteoZip, being similar to HA/BG, exhibited better osteogenic differentiation than BG did, shown by augmented differentiation marker activity at both protein and mRNA levels. Sandwich ELISA was used to quantify angiopoietin and inducible nitric oxide synthase which are involved in peri-prosthetic angiogenesis and aseptic loosening of total hip replacement, respectively. Both Bioglass-derived coatings provide superior initial osteoconductivity to OsteoZip, and HA/Bioglass composite coating outruns in long-term osteogenic differentiation and prognostic bioprocesses. The novel coatings discovered in this study have significant potential in providing both orthopedic and therapeutic functions.

Biotechnol. Bioeng. 2011;108: 454–464.

© 2010 Wiley Periodicals, Inc.

KEYWORDS: bioactive glass; growth factors; osteoconduction; hydroxyapatite coating; mRNA

Introduction

Bioactive glass and hydroxyapatite (HA) are two of the most commonly used bioactive ceramics for hard tissue repair (Best et al., 2008). They share similar clinical applications including tooth implant in dental surgery, ossicular reconstruction in otolaryngological surgery, bony restoration in maxillofacial surgery, and vertebra prostheses in spinal surgery (Hench, 1991, 1998; Park, 2008). However, they possess different popularity in the field of orthopedic surgery (Kokubo, 2008): Bioactive glass is generally used as a bone graft for osseous defects in non-load-bearing sites, whereas HA is a favorable coating for metal implants used in load-bearing scenario, for example, HA-coated Titanium (Ti) alloy as the femoral stem of a total hip replacement (THR). Bioactive glass and HA also differ in their bioactivity upon contact with host bone tissue. HA is usually considered osteoconductive as osteoblasts are able to attach, grow, and differentiate on it (Albrektsson and Johansson, 2001). Apart from its anti-microbial and anti-inflammatory feature, bioactive glass performs at a higher level being considered osteostimulative, due to its ability to stimulate growth factor production in addition to osteoconductivity (Hu and Zhong, 2009).

The underlying rationale of using a coated implant for THR is to combine the mechanical strength of relatively weak HA so that the long-term stability of the implanted prosthesis can be achieved (Landor et al., 2007). Although there are many well-developed methods for coating HA onto orthopedic implants (Narayan, 2009), fewer processes have been successful in applying bioactive glass onto such implants (Yafan et al., 2005), very limited amount of work has touched upon the biocompatibility of bioactive coating

Correspondence to: Mohamed Al-Rubeai
Contract grant sponsor: Science Foundation Ireland
Contract grant number: 08/SRC/11411

(Foppiano et al., 2007), but no comparison with HA coating was carried out in vitro in terms of osteoconductivity. CoBlast™ (O'donoghue and Haverty, 2008), a promising novel coating process, has shown to effectively create a HA coating on a Ti substrate (O'Neill et al., 2009) with excellent in vitro osteoconductivity and in vivo osseointegration (O'Hare et al., 2010). This cost-effective and transferrable process has been used to produce a bioactive glass interface in this study using the first bioglass composition, 45S5 Bioglass® (BG) discovered by Larry Hench 40 years ago (2006). The resultant surfaces, BG and HA/BG, are characterized and the results are correlated with in vitro cellular data, and compared with the standard HA surface created with same technique, commercially known as OsteoZip™. In vitro osteoconductivity has been evaluated in terms of cell attachment, proliferation, and differentiation at both protein and mRNA level by using osteosarcoma MG63 cells which produce phenotypic osteoblast markers and growth factors (Kieswetter et al., 1996; Zinger et al., 2005).

Angiopoietin (Ang) and inducible nitric oxide synthase (iNOS) expression have been studied in this work due to their involvement in a major post-THR complication: aseptic implant loosening (Sargeant and Goswami, 2006). Inflammatory osteolysis (Abu-Amer et al., 2007) and diminished angiogenesis (Santavirta et al., 1996) are two primary mechanisms of aseptic implant loosening. Nitric oxide (NO) and its predominant producer iNOS have significant roles in peri-prosthetic osteolysis (Puskas et al., 2003), while Ang-1 promotes the remodeling, maturation, and stabilization of blood vessels (Holash et al., 1999). Analysis of the levels of individual indicators and the possible connection between them has been performed. Basic fibroblast growth factor (bFGF) has an autocrine role during bone formation (Bodo et al., 2002), and studying its temporal expression has prompted a better understanding of osteoblast behavior on the biomaterials.

Materials and Methods

Production and Characterization of CoBlast Coatings

After Ti-6Al-4V alloy substrates, sized 15 mm × 15 mm × 1 mm, were cleaned by 15 min sonication each in HCl and IPA, the three surface interfaces were created via the CoBlast process (EnBIO Cork, Ireland). In brief, dopant and abrasive were simultaneously blasted through separate nozzles at different pressures (Table I). All samples underwent post-

CoBlast cleaning by sonication for 1 min in IPA. They were then stored in a desiccator (Lennox, Dublin, Ireland) until autoclaved at 121°C for 20 min prior to experiments. Optical profilometry (Wyko NT1100, Veeco, Cambridge, UK) was carried out on the interfaces to obtain surface roughness values. Hydrophilicity, expressed as water contact angle, was measured via the sessile drop method using a video-based contact angle meter (OCA 20, Dataphysics, Filderstadt, Germany).

Cell Culture

Human MG63 osteoblastic cells (ATCC, Middlesex, UK) from passages 8 to 12 were used for all cellular experiments. They were cultured at 37°C in a humidified 5% CO₂ atmosphere in a complete culture medium containing 88% (v/v) Dulbecco's modified Eagle's medium (DMEM), 10% fetal bovine serum, 1% L-glutamine, and 1% penicillin/streptomycin. All reagents above were from Sigma-Aldrich (Dorset, UK). Cells were sub-cultured every 2 days at 80% confluency. All cellular studies were carried out in 12-well tissue-culture plate (OrPlate, Orange Scientific, Braine-l'Alleud, Belgium) where each sample was immersed by 1 mL cell growth medium.

Protein Adsorption

Surfaces were conditioned by incubation for 5, 10, 20, 40, and 80 min in complete medium at 37°C in 5% CO₂ incubation. At different time points samples were gently washed with deionized (DI) H₂O and proteins were desorbed by immersing samples separately in 6 M urea for 3 h at 37°C. Protein content was then quantified using the QuantiPro™ bicinchoninic acid (BCA) protein assay kit (Sigma-Aldrich) based on supplier's protocol.

Cell Attachment and Morphology

MG63 cells were seeded onto the surface at a concentration of 8 × 10⁵ cells/mL. This relatively high concentration was used to saturate the bonding capacity of each surface to prevent falsely low results. Cells were cultured as described previously for up to 200 min. At the end of each time point (25, 100, and 200 min), samples were moved to new 12-well tissue-culture plates and washed twice with Dulbecco's phosphate-buffered saline (DPBS, Sigma, Dorset, UK). Cells were then detached with Accutase™ and counted using

Table I. CoBlast parameters for depositing three surfaces.

Surface designation	Dopant (Do)	Abrasive (Ab)	Pressure Do/Ab (psi)	Nozzle angle Do/Ab (°)	Nozzle height Do/Ab (mm)	Speed (mm/s)
BG	BG	MCD-180	75/75	82/78	8/16	13/15
HA/BG	HA	BG	75/75	82/78	8/16	13/15
OsteoZip	HA	MCD-180	90/75	82/78	8/16	13/15

CyQUANT[®] Direct assay which is based on a cell-permeant DNA-binding dye in combination with background suppression reagents.

Attached cells from the other replicate were fixed with 2.5% (w/v) glutaraldehyde for 30 min at 4°C followed by dehydrating with a series of ethanol/H₂O solutions with increasing ethanol concentration (30%, 50%, 70%, 80%, 90%, 95%, and 100%). Samples were finally treated with 1 mL hexamethyldisilazane (HMDS) for 1 min, left for air dry at room temperature and stored in a desiccator. Samples were coated with gold by a turbo pumped high-resolution sputter coater (K575X, EmiTech, Kent, UK) before being examined under scanning electron microscope (SEM, Quanta[™] 3D FEG, FEI[™], Cambridge, UK) which was operating at 5 kV and 6.66 pA with an observation angle at 52°.

Immunocytochemical Staining

After 18 h of culture, cells were fixed in situ with 4% (w/v) paraformaldehyde DPBS solution, gently washed twice with wash buffer containing 0.05% (v/v) Tween-20, permeabilized with 0.1% (v/v) Triton X-100 solution, and blocked with 1% (w/v) BSA DPBS solution. One percent (v/v) primary anti-Vinculin antibody was added and incubated for 1 h, and 1% (v/v) fluorescein isothiocyanate (FITC)-conjugated secondary antibody was incubated simultaneously with 1% tetramethylrhodamine isothiocyanate (TRITC)-conjugated phalloidin. Each staining step above was followed by five 8-min washing steps, and all reagents above were from the actin cytoskeleton and focal adhesion staining kit (Millipore, Watford, UK). Stained cells were observed using a confocal laser scanning microscope (CLSM, Zeiss LSM 510 Meta, Carl Zeiss Ltd, Hertfordshire, UK).

Ionic Dissolution

Each surface was submerged in 3 mL complete cell growth medium in a 12-well tissue-culture plate, and was placed in a 37°C cell culture incubator. The concentrations of released ions of silicon (Si), calcium (Ca), and phosphorous (P) in the complete medium were measured by inductively coupled plasma optical emission spectroscopy (ICP-OES, Vista-MPX, Varian, Oxford, UK) on days 1, 3, 5, 7, 9, and 11, respectively. This was to coincide with periods of media renewal for MG63 cells.

Cell Proliferation

Cells were seeded onto the surface at a density of 8×10^4 cells/mL. This relatively low concentration was chosen to prevent an early confluency to facilitate a cell growth curve with more time points. After 24 h, samples were moved to a new 12-well tissue-culture plate, gently rinsed with warm DPBS, and immersed in fresh medium. At each time point (days 1, 3, 5, and 7), cell proliferation was

measured using the alamarBlue[®] assay (Invitrogen, Paisley, UK) which is an in situ, non-toxic metabolic assay (Tierney et al., 2009). In brief, 10% (v/v) alamarBlue[®] reagent was aseptically added to cells in existing media and incubated at 37°C for 3.5 h. One hundred microliters of the homogenized supernatants were placed in triplicate into a 96-well plate, and the absorbance read on a microplate reader (GENios[™], TECAN, Reading, UK) at 570 nm normalized to 600 nm. Cell number was calculated based on a standard curve.

Differentiation Markers Activity

The attached cell layer was lysed (Morris et al., 1992) and extracted protein was solubilized by a cell lysis/extraction reagent (CellLytic[™] M, Sigma) on a gyratory rocker (Stuart[®] SSL3, Essex, UK). A colorimetric assay (SensoLyte[®] ALP assay kit, AnaSpec, Cambridge, US) based on dephosphorylation of *p*-nitrophenyl phosphate (*p*NPP) by alkaline phosphatase (ALP) (EC 3.1.3.1) was used. Color change of *p*NPP was directly proportional to ALP activity and its absorbance was detected at 405 nm. Total intracellular protein was quantified using a BCA protein assay kit (Sigma-Aldrich).

The production of osteocalcin (OC) in supernatants was determined colorimetrically using an immunoenzymatic assay (Invitrogen) employing highly specific monoclonal antibodies and horseradish peroxidase-labeled OC.

Reverse Transcription PCR (RT-PCR) and Real-Time PCR (Q-PCR)

On day 15, RNeasy[®] Plus Mini kit (QIAGEN, West Sussex, UK) was used to purify RNA from harvested cells without the need for additional DNase digestion. In brief, cells were lysed and homogenized, the lysates were passed through a genomic DNA eliminator spin column, and ethanol was added prior to transfer to an RNeasy spin column. The integrity and size distribution of total RNA was checked by using an Agilent 2100 Bioanalyzer and RNA 6000 Nano chip (Agilent Technologies, Cork, Ireland). RNA purity and concentration was determined using a NanoDrop[™] spectrophotometer (ND-1000, Thermo Scientific, Surrey, UK). First-strand complementary DNA (cDNA) was synthesized from 2.8 µg RNA for each sample using oligo(dT)₁₂₋₁₈, dNTP mix and SuperScript[™] II reverse transcriptase (Invitrogen).

Q-PCR was performed on the 7900HT Fast Real-Time PCR System using TaqMan[®] Gene Expression Assays (Applied Biosystems, Cheshire, UK) for assessing the expression of bone and extracellular matrix (ECM)-related genes using 18S as an endogenous control (Table II). A 384-well plate with 10 µL reaction mixture per well containing 0.5 µL target gene, 0.5 µL 18S, 0.5 µL cDNA, 5 µL TaqMan[®] Universal PCR Master Mix, and 3.5 µL H₂O was used. cDNA samples derived from three independent cultures and were run in duplicate. PCR conditions were

Table II. Target genes and endogenous control gene used for real-time PCR.

Gene symbol	Gene name	RefSeq	Assay ID	Amplicon length
<i>ALPL</i>	Alkaline phosphatase	NM_000478.3	hs01029144_m1	79
<i>BGLAP</i>	Osteocalcin	NM_199173.3	hs00609452_g1	74
<i>COL1A1</i>	Type I collagen	NM_000088.3	hs00164004_m1	66
<i>18S</i>	18S rRNA	X03205.1	4310893E	187

Primers sequences are proprietary to Applied Biosystems; however, assays are reproducible provided they have same assay IDs.

as follows: activation (50°C for 2 min and 95°C for 10 min) followed by 40 amplification cycles (95°C for 15 s and 60°C for 1 min). The relative expression level, expressed as a fold change, was obtained using the $2^{-\Delta\Delta C_T}$ method as previously described (Livak and Schmittgen, 2001). Cells grown on the same polystyrene 12-well tissue-culture plate as previously described were chosen as control to facilitate the calculation of $2^{-\Delta\Delta C_T}$ method.

Collagen Content and Cell Detachment

Total collagen released into the culture medium was determined quantitatively using the SircolTM soluble collagen assay (Biocolor, Carrickfergus, UK) which is based on the binding of a dye, Sirius Red, to the intact triple helix organization of native collagens. One hundred microliters of day 15 cell culture supernatants were mixed in triplicate with Sircol dye reagent, centrifuged to form pellets of collagen-dye complex and unbound by an alkali reagent. The absorbance of dissolved dye was measured at 540 nm, and compared to the standard curve generated according to collagen Type I.

On day 15, multilayers of cells cultured for 15 days was prepared for SEM as previously described except that cells were dried by HMDS within an operating fume hood to accelerate the evaporation of HMDS. Cells from the same time point were washed using DPBS and detached by Accutase. They were then carefully collected at each time point and counted, values were divided by the pre-detachment cell count (determined by alamarBlue assay) to obtain the percentage of detached cells. Cell viability is still >95% after 20 min contact with Accutase (data not shown).

Growth Factors and Enzyme Level

Ang-1, Ang-2, and bFGF concentration was measured by their secretion level in cell culture supernatants, whereas intracellular iNOS (EC 1.14.13.39) was measured from cell lysates. They were individually quantified by sandwich enzyme-linked immunosorbent assay (ELISA) using Quantikine[®] colorimetric ELISA kits (R&D Systems, Abingdon, UK). In brief, samples were pipetted into the wells of a microplate pre-coated by analyte-specific capture antibody. The captured analyte was then bound to enzyme-linked detection antibody. A substrate solution was added

and color developed in proportion to the amount of analyte bound initially. The color development was stopped and the intensity of the color was measured at 450 nm by a plate reader. NO level was measured by determining the accumulation of its primary and stable oxidized product, nitrite (Green et al., 1982). Griess reagent (Sigma) was added to react with nitrite to yield a purple azo derivative. The absorbance of the resultant solution was measured at 540 nm. A standard curve based on sodium nitrite was used to calculate total nitrite concentration.

Statistical Analysis

Data are expressed as mean \pm standard deviation from five independent material characterizations and three independent cellular experiments. Group data were compared using one-way analysis of variance, and if significant, data from each surface was compared using the Student's *t*-test. *P*-value <0.05 was considered significant. All statistical calculations were implemented using SPSS Statistics 18 (IBM[®], Chicago, IL).

Results and Discussion

Surface Characteristics, Protein Adsorption, Cell Attachment, and Cell Adhesion

Prior to cellular experiments, two essential material characteristics: surface roughness and hydrophilicity were quantified by profilometry and goniometry, respectively (Table III). Surface roughness does not differ significantly, except that OsteoZip is slightly rougher than HA/BG. The R_a values of BG and HA/BG coatings are in line with those in Choi's (2009) and Koller's (2007) studies using bioactive glass as abrasive for Ti surfaces. Although all surfaces are hydrophilic (water contact angle <90° is hydrophilic and >90° is hydrophobic), their hydrophilicity differs significantly ($P < 0.001$), with BG being most hydrophilic and OsteoZip least hydrophilic. Both material parameters can influence cell attachment by affecting protein adsorption (Anselme, 2000). Results of X-ray diffraction (XRD), X-ray photoelectron spectroscopy (XPS), mechanical scratch test, and cross-section transmission electron microscopy (TEM) have been submitted elsewhere.

Table III. Average surface roughness (R_a) and water contact angle.

Surfaces	R_a (μm)	Contact angle ($^\circ$)
BG	1.01 ± 0.16	9.1 ± 0.5
HA/BG	0.92 ± 0.08	12.5 ± 0.7
OsteoZip	1.18 ± 0.11	40.2 ± 1.5

Cell attachment to biomaterials follow a general sequence: protein adsorption to the surface, cells sense the thin protein layer, cells attach and orientate, and cells grow to form tissue (Paital and Dahotre, 2009). Thus, the adsorption of proteins plays a crucial role in tissue–implant interaction. Distinct protein adsorption kinetics can be found in Figure 1A in which the total amount of adsorbed protein demonstrates a clear sequence: BG > HA/BG > OsteoZip ($P < 0.001$). The differences between BG and OsteoZip, and between BG and

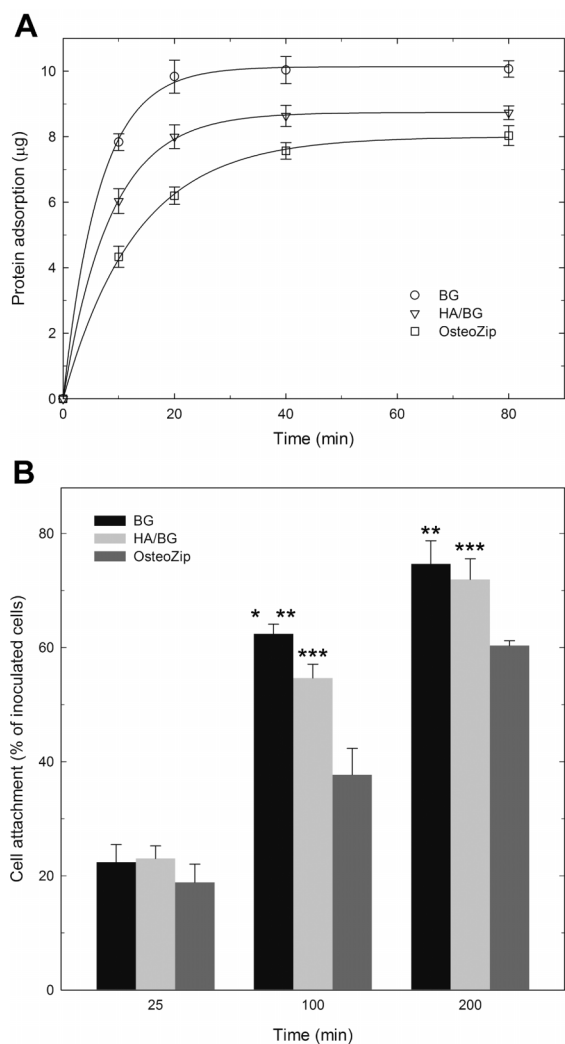


Figure 1. **A:** Protein adsorption to the surfaces up to 80 min. Exponential curves were fit to the data points. **B:** Quantitative assessment of MG63 cell attachment to the surfaces up to 200 min. Statistical difference exists when BG versus HA/BG (*), BG versus OsteoZip (**), and HA/BG versus OsteoZip (***).

HA/BG, are most likely due to the differences in their hydrophilicity. The difference between HA/BG and OsteoZip on the other hand, is likely a net result of roughness and hydrophilicity as proposed by Wang et al. (2008): higher surface roughness (thus larger surface area) and lower hydrophilicity are competitors towards the final amount of adsorbed protein.

The resultant cell attachment is manifested quantitatively (Fig. 1B) and qualitatively (Fig. 2). In Figure 1B, attached cell numbers generally increase with time. Similar amount of cells are attached to each surface at 25 min, after which cell attachment differs significantly ($P < 0.001$). Cell attachment follows the same trend as protein adsorption except that at 200 min, a similar amount of cells are attached to BG and HA/BG. Irrespective of surface difference, more than 60% of seeded cells have already attached by 200 min.

The morphology of representative cells attached onto each surface at each time point is displayed in Figure 2. Sequential changes in cell morphology pre- and post-contact with the surface consist of the following stages: a spherical shape in the medium, point contact with the surface, centrifugal growth of filopodia, extension of lamellipodia, and flattening of the cell (Rajaraman et al., 1974). This sequence is well proven on each surface although at the same time point, cells on different surfaces have different appearances. Cells on all surfaces are spherical with early development of filopodia at 25 min, with cells on BG being the first to loosen their base by creating early lamellipodia. Differences in cell morphology are emphasized at 100 min when cells on OsteoZip still possess a spherical body but cells on BG have more extensive lamellipodia and a fairly flattened architecture. By 200 min, cells on all surfaces have significantly transformed, especially on BG and HA/BG where cells begin to orientate by becoming polygonal. From this point on, cell morphology does not change substantially with time (Fig. 3D) which means cell attachment on BG and HA/BG stabilizes within 200 min. From the above quantitative and qualitative results one can conclude that cell attachment is faster and more advanced on BG-derived surfaces.

Cell adhesion, expressed as distribution of actin filaments and vinculin focal adhesion, was assessed by CLSM 18 h after inoculation when cells on all surfaces are similarly settled (Fig. 3D). Cells on all surfaces seem to have a similar actin organization (Fig. 3A–C) with highly tensioned actin bundles visualized, although cells on BG have a more delicate actin network containing both cortical and radial fibers. Extreme differences in the vinculin focal adhesion pattern were observed (Fig. 3a–c). BG and HA/BG have cells with fine dot-like vinculin-containing focal adhesion plaques seen along the entire edge of the cells where the strongest bond with the material is, whereas focal contact with OsteoZip is much less. Thus, cell adhesion is better on BG-derived surfaces. It has been shown previously that more hydrophilic surface tends to have better cell attachment and cell adhesion (Anselme, 2000; Paital and Dahotre, 2009). This might indicate their potential to provide early

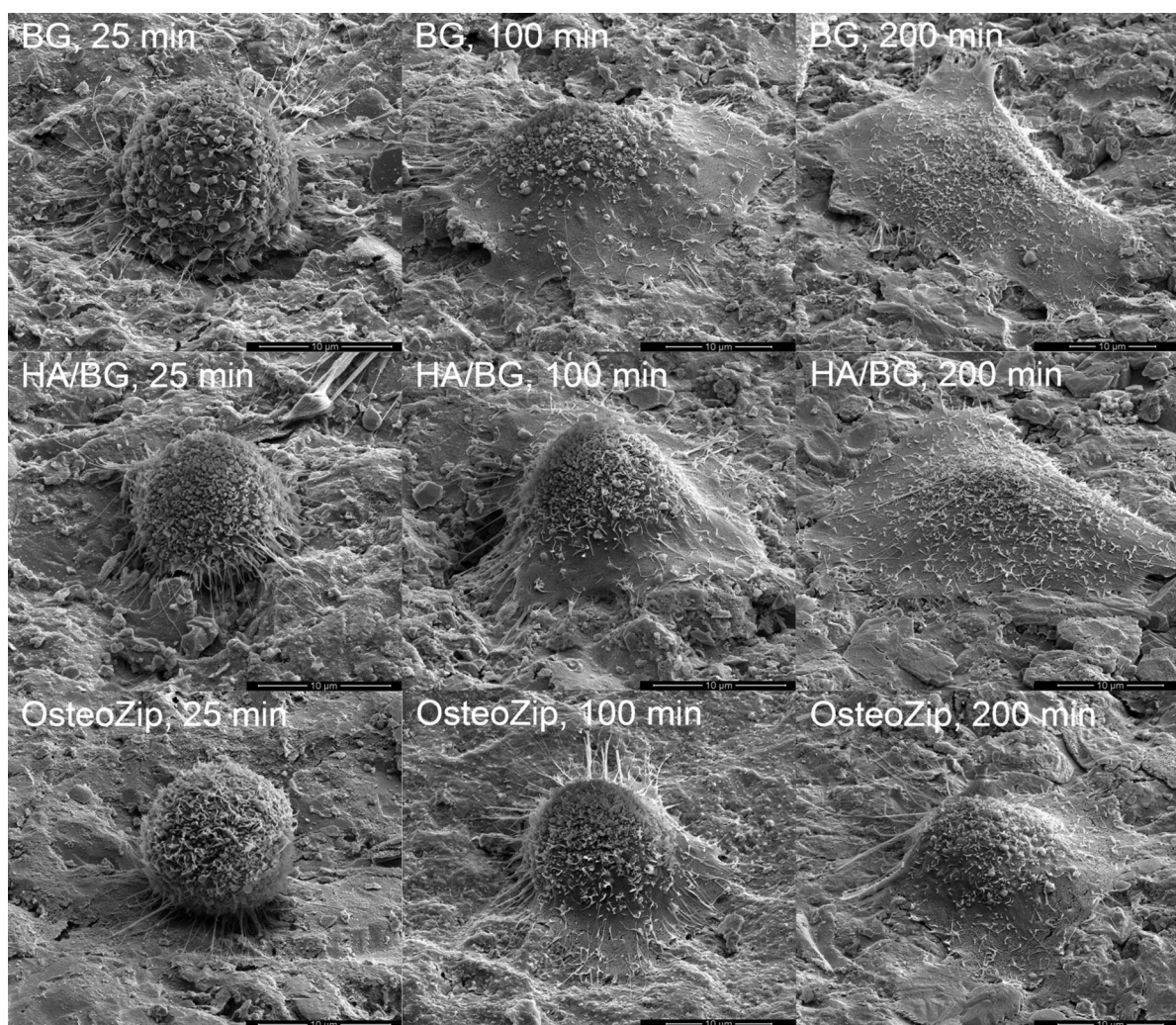


Figure 2. SEM images of MG63 cell morphology on each surface at 25, 100, and 200 min. Columns and rows correspond to incubation time and surface type, respectively. Scale bar = 10 μm .

osseointegration (Cooper et al., 1998) which is a crucial state for the success of both orthopedic and dental implantation.

Ion Dissolution and Cell Proliferation

The osseointegration of bioactive glass after implantation has been attributed to the precipitation of a carbonated apatite layer on the glass surface at the expense of dissolution of ions upon contact with body fluid (Kokubo, 2008). HA dissolves as well in physiological fluid but at a much slower rate due to its crystallinity. In this work, Si, Ca, and P ions released into complete cell growth medium were monitored by ICP-OES over a 7-day period (Fig. 4A). The dissolution behavior of OsteoZip is expected: Ca and P levels were maintained around the baseline for 7 days except for a slight increase on day 1, while [Si] equals that in the medium as HA does not contain Si. This result is consistent with recent

findings (O'Neill et al., 2009) and is likely due to the near 100% crystallinity of the HA surface deposited by the CoBlast process.

Both Bioglass-derived surfaces have significant release of Ca and Si but showed a slight drop of P levels at a similar extent 1 day after immersion. The mechanism of this ion release has been thoroughly categorized (Kokubo, 2008). At day 1, [Ca] in BG and HA/BG culture systems parallel each other except for a slightly higher [Ca] in BG on day 3. [P] increases on day 3 and subsequently returns to baseline levels. An interesting finding of [Si] is noted with higher [Si] levels in BG than in the HA/BG culture system on day 3 with the reverse occurring on days 5 and 7. This probably suggests that HA/BG provides slower release of Si in vitro, and potentially a more persistent release in vivo. One can postulate that the CoBlast procedure itself most likely contributes to this difference as Bioglass was used as a dopant and abrasive in BG and HA/BG, respectively. In

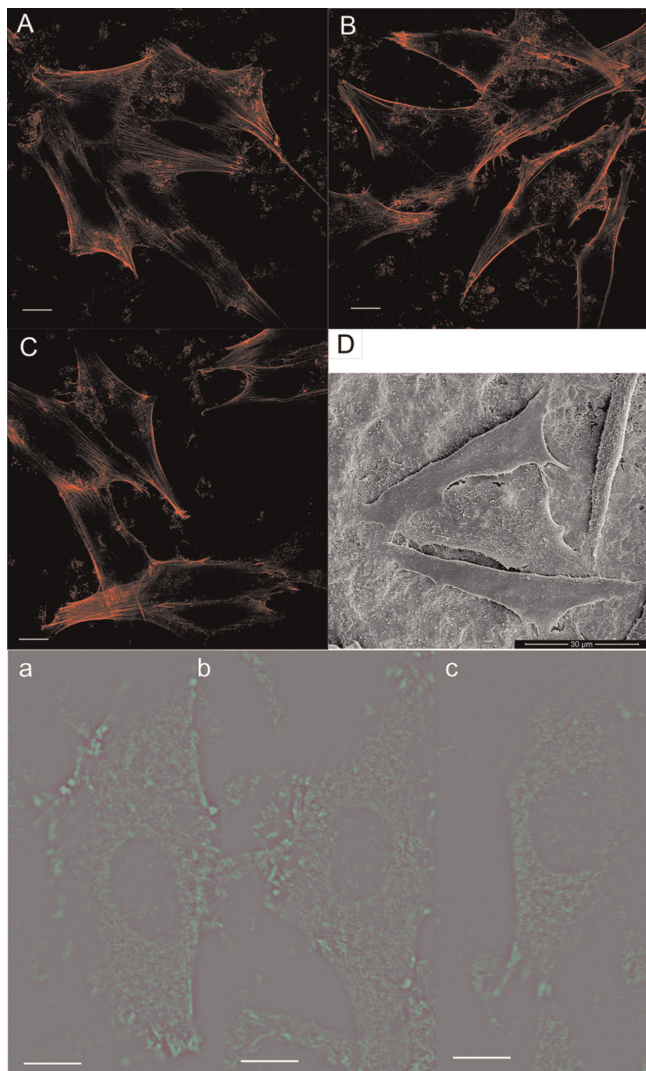


Figure 3. CLSM images of actin cytoskeleton (A–C) and vinculin focal adhesion (a–c) of MG63 cells on each surface 18 h after inoculation, scale bar = 10 μm . SEM image (D) represents the general morphology of cells attached after 18 h, scale bar = 30 μm . [Color figure can be seen in the online version of this article, available at wileyonlinelibrary.com.]

comparison to the bioactive glass coating generated by plasma-spray technique (Lee et al., 1996), our Bioglass-based coatings have similar P ion release pattern but a slower release of Si and Ca ions. This is encouraging as more hydroxycarbonate apatites are expected to be precipitated on these coatings. Since a tremendous amount of research has been carried out in the pursuit of a controlled and balanced dissolving of coating in THR (Narayan, 2009), the underlying mechanism of our finding in ion dissolution is worth exploring in the future.

Cell proliferation was monitored using an in situ alamarBlue™ assay until the end of the first week (Fig. 4B). There is no significant difference in cell number between each surface after 24 h of culturing ($P > 0.05$). From day 3 onwards, cell numbers on BG and HA/BG are

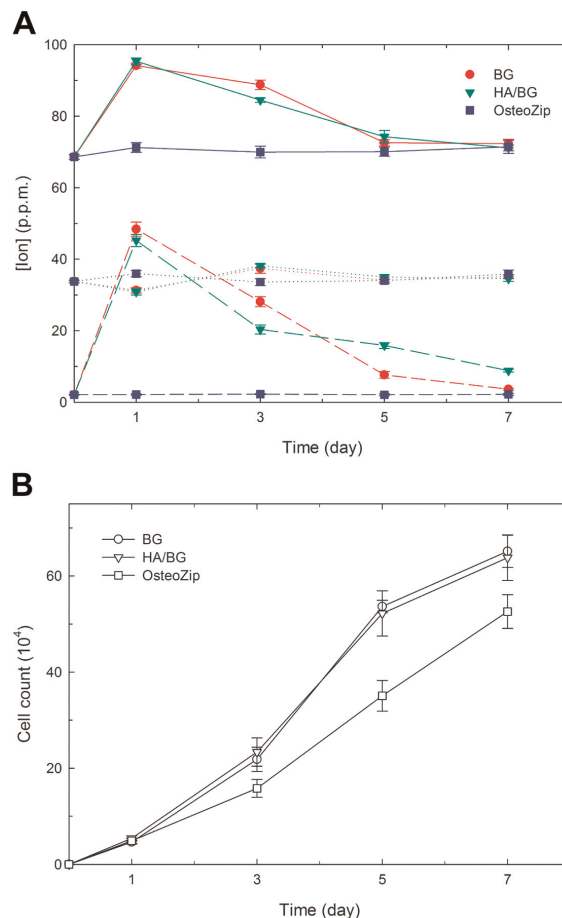


Figure 4. A: Ion dissolution of Si, Ca, and P from BG, HA/BG, and OsteoZip in complete cell growth medium up to day 7. Straight line, Ca; dotted line, P; broken line, Si. The baseline ion concentration in cell growth medium was measured and expressed at day 0. B: MG63 cell proliferation during 7 days culture. [Color figure can be seen in the online version of this article, available at wileyonlinelibrary.com.]

similar, but are higher ($P < 0.001$) than that on OsteoZip at each time point. Cell proliferation seems to be faster on BG-derived surfaces. This is not surprising as dissolution products alone from Bioglass are sufficiently stimulative on cell proliferation by shifting cells into the S phase of the cell cycle (Hench, 2006; Sun et al., 2007; Xynos et al., 2000).

Cell Differentiation and Cell Detachment

Confluent proliferating cells subsequently enter the differentiation phase, with the expression of the most common biochemical markers including ALP, type I collagen, and OC (Bilezikian et al., 2008). In this work, after over 2 weeks of differentiation, there is no significant difference in ALP levels (Fig. 5A). That is likely due to the role of ALP as an early differentiation marker (Bilezikian et al., 2008), with cells on all surfaces having already passed the initial differentiation stage by the end of week 2. Collagen production on BG is nevertheless, significantly lower than

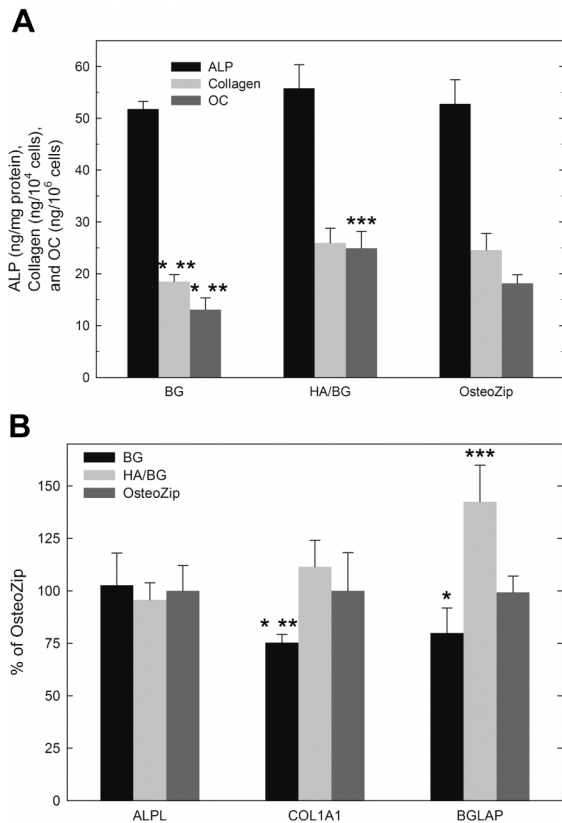


Figure 5. **A:** ALP, collagen, and OC levels in the differentiation stage of MG63 cells. ALP is expressed intracellularly, and collagen and OC are secreted into supernatant, thus their results are normalized to intracellular total protein content and total cell number, respectively. **B:** mRNA expression of bone- and extracellular matrix-related genes at day 15. Gene expression is shown relative to the mean percentage found in OsteoZip. *ALPL* gene encodes ALP, *COL1A1* gene encodes collagen type I, and *BGLAP* gene encodes OC, respectively. Statistical difference exists when BG versus HA/BG (*), BG versus OsteoZip (**), and HA/BG versus OsteoZip (***).

that on HA/BG and OsteoZip ($P < 0.05$). Osteocalcin, a late marker of osteogenic differentiation is expressed differentially on all surfaces: HA/BG > OsteoZip > BG ($P < 0.01$ BG vs. HA/BG, rest $P < 0.05$). This indicates that osteogenic differentiation is most advanced on the HA/BG surface, but is most immature on the BG surface. In order to verify this finding at the mRNA level, RT-PCR and real-time PCR was conducted on three genes which translate into the proteins mentioned above.

Figure 5B shows the mean expression level of target genes, from three independent experiments, as a percentage of OsteoZip. *ALPL* expression does not differ significantly amongst surfaces ($P > 0.05$). Expression of *COL1A1* in HA/BG and OsteoZip is similar, but both are higher than that of BG ($P < 0.05$). Although cells on BG and OsteoZip express *BGLAP* at comparable levels, HA/BG is almost double BG's gene expression ($P < 0.001$) despite the fact they are both BG-derived surfaces. In general, gene expression is consistent with the transcribed protein content.

Irrespective of BG's enhanced performance in early stages (cell attachment and cell proliferation), it is not as supportive as OsteoZip in terms of osteogenic differentiation. Encouragingly, HA/BG surpasses OsteoZip in most aspects of osteoconductivity. This is not surprising as it has been previously shown that gel-derived HA/BG composites demonstrated better bioactivity and biocompatibility compared to HA alone (Cholewa-Kowalska et al., 2009).

Cell detachment by Accutase™ was implemented to confirm collagen robustness in a multilayer of cells on the surface at day 15. Collagen is the most abundant protein in ECM which is the defining feature of connective tissue in vivo. Accutase is a routine cell detachment solution of collagenolytic enzymes. At 10 min, more than half of the cells are detached from BG surfaces (Fig. 6D), although over 60% of cells still remain attached to the HA/BG and OsteoZip surfaces ($P < 0.01$). This difference minimizes at 20 min as nearly complete detachment of cells are seen from all surfaces, and this is consistent with reported efficiency of Accutase. Due to the significant difference in cell detachment at 10 min, it could be faster for Accutase to detach cells from BG surfaces than HA/BG or OsteoZip surfaces.

SEM images (Fig. 6A–C) present the morphology of cell layers at day 15. Well orientated and packed cell layers can be observed on all surfaces, although large and deep gaps spread across the cell layer on BG surface. During the final drying stage by HMDS, the fume hood was running at the maximum speed (see the Materials and Methods Section). Our internal study has demonstrated that this procedure, compared to drying samples under windless environment, tend to induce crack-like artifact, only within multilayer of cells on BG surface. BG cell layers contain less collagen content within the ECM connecting cells and cell layers, thus, it is more vulnerable to vigorous drying. Again, both the detachment assay and cell layer morphology have verified the collagen quantification.

bFGF Expression During Cell Proliferation and Differentiation

ELISA was conducted to quantify bFGF concentration in supernatants at days 3 and 15. Cells secrete significantly higher levels ($P < 0.001$) of bFGF at day 3 than at day 15 regardless of different surfaces (Fig. 7A). bFGF is more abundant in the BG than in OsteoZip culture system ($P < 0.05$) at both time points; however, its levels in the HA/BG system shifts from paralleling the BG culture at day 3 to paralleling the OsteoZip culture at day 15. Careful explanation of results is necessary here as bFGF is an autocrine growth factor controlling in vitro bone formation (Bodo et al., 2002). In brief, bFGF stimulates bone cell replication but inhibits differentiation-related markers (Bilezikian et al., 2008). If this is taken into account, the bFGF expression considerably matches the cell proliferation and differentiation results discussed above. Better proliferation on BG and HA/BG is consistent with the higher bFGF

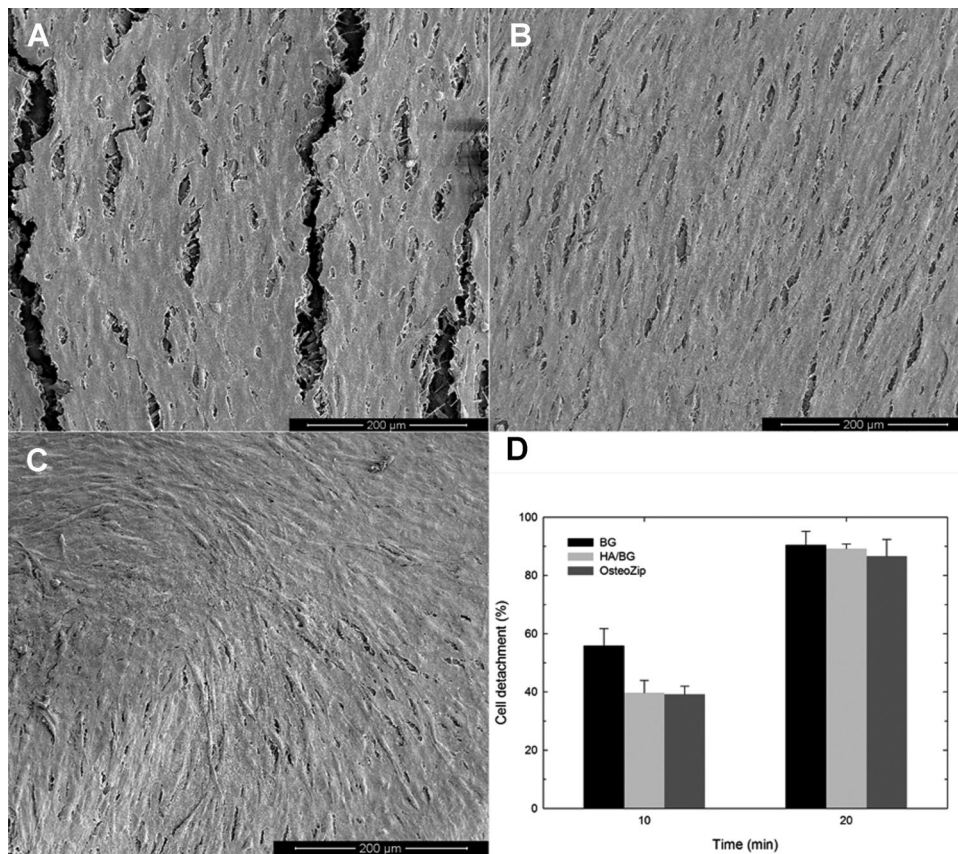


Figure 6. SEM images of cell layer morphology (A, BG; B, HA/BG; C, OsteoZip, scale bar = 200 μm) after 15 days of culture, and cell detachment (D).

secretion level of cells on these surfaces, while more advanced osteogenic differentiation on HA/BG and OsteoZip is consistent with the lower bFGF secretion level of cells. Due to CoBlast's potential to deposit unaltered therapeutic and bioactive agents (O'Hare et al., 2010), the result here could potentially facilitate our designing a THR coating with controlled release of growth factor resulting in an in vivo influence beyond bone formation, as bFGF is associated with bone remodeling, osteoporosis, and regulation of other growth factor production (Bilezikian et al., 2008).

Ang-1, Ang-2, iNOS, and NO Levels

As briefly mentioned in the introduction, Ang and iNOS can be ultimately linked to aseptic implant loosening through different mechanisms. Ang-1 and Ang-2 are two types of angiopoietin which are angiogenic regulating protein growth factors constitutively expressed in bone and vascular tissues (Lewinson et al., 2001; Liekens et al., 2001). Ang-2 is a naturally occurring antagonist of Ang-1 (Liekens et al., 2001) as Ang-1 and Ang-2 both bind the same receptor but only Ang-1's binding results in signal transduction and

regulation of blood vessel maturation. Ang-1 secretion (Fig. 7B) is seen at three distinct levels: with HA/BG being the highest, BG being the lowest and OsteoZip in the center ($P < 0.01$). Ang-2 levels, on the other hand, are too low to be detected in HA/BG and OsteoZip cultures (ELISA for Ang-2 has a sensitivity of 8.3 pg/mL), but is successfully detected in BG culture. Thus, HA/BG has the best angiogenic potential among the three surfaces, with the traditional HA surface, OsteoZip, more likely to have better peri-prosthetic vascularization than BG.

Figure 7C demonstrates the enzyme activity of iNOS and the synthesis of its product NO. A reverse trend to the above Ang results is noted in this data. Values of the three cultures are in a decreasing order: BG > HA/BG > OsteoZip, which applies to both iNOS ($P < 0.01$) and NO results ($P < 0.05$) except that OsteoZip's NO production almost levels that of HA/BG ($P > 0.05$). As for that, long-term exposure of peri-implant tissue to NO with an intrinsic stimulus is likely going to render BG-coated implants more susceptible to loosening from the host, resulting in a failure of the THR (Puskas et al., 2003).

A positive connection between Ang-1 and osteoblast metabolism, bone formation and bone regeneration after operation has been established (Horner et al., 2001;

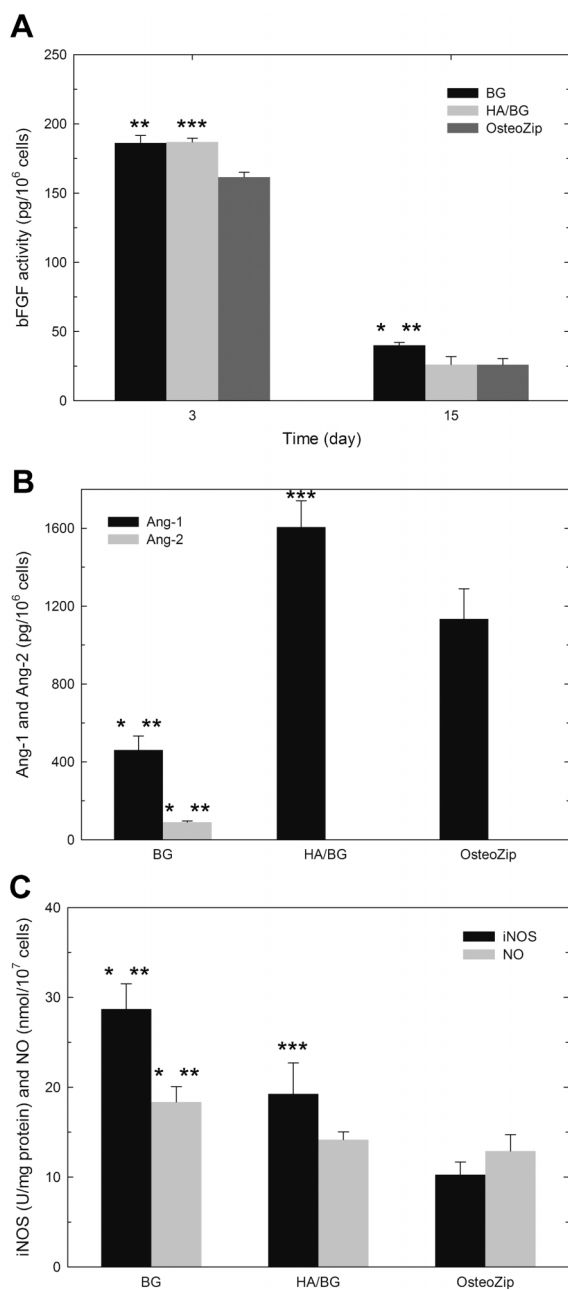


Figure 7. A: bFGF production in proliferation and differentiation stages. B: Ang-1 and Ang-2 secretion at day 21. C: Intracellular iNOS production and extracellular NO level at day 21. Statistical difference exists when BG versus HA/BG (*), BG versus OsteoZip (**), and HA/BG versus OsteoZip (***)

Lewinson et al., 2001). In addition, Ang-based therapeutics have already been applied in vivo for accelerating bone formation after orthopedic procedures and ameliorating orthopedic complications (Park et al., 2009, 2010). Kasama et al. (2007) suggested a negative association between Ang-1 and iNOS seen in the inhibitory effects by tumor necrosis factor-alpha and interferon-gamma. The in vitro results of Ang and iNOS in this study are more than likely related.

Considering all of the above findings, one can propose that maximizing the beneficial clinical features (e.g., angiogenesis by angiopoietin) and minimizing adverse stimuli (e.g., iNOS and NO) from the surface might represent the new direction for coating design and manufacturing.

Conclusions

Newly developed Bioglass surfaces using the CoBlast technique have been compared with HA coating in terms of osteoconductivity and growth factor production. Both Bioglass-derived surfaces have great potential as they exhibited better performance than HA in early stages of cell-material interaction, that is, cell attachment and cell proliferation. However, HA/BG composite coating is most likely the best among all three coatings as it has been proven to be persistently superior to HA and BG with regard to both cellular response and biochemical stimulation. Within the limits of this investigation, it can be concluded that the reported Bioglass coatings for orthopedic and dental implants are significant boosts to the current clinical standards. In addition to that, the underlying coating technique has the potential to provide a platform to produce more cost-effective and clinically potent implant coatings.

This work was supported by Science Foundation Ireland (grant no. 08/SRC/11411). The authors would like to thank EnBIO (Cork, Ireland) for providing CoBlast samples. Acknowledgement also goes to staff and postgraduate students of Surface Engineering Group led by Dr. Denis Dowling, University College Dublin, Ireland.

References

- Abu-Amer Y, Darweh I, Clohisy J. 2007. Aseptic loosening of total joint replacements: Mechanisms underlying osteolysis and potential therapies. *Arthritis Res Ther* 9 (Suppl 1):S6.
- Albrektsson T, Johansson C. 2001. Osteoinduction, osteoconduction and osseointegration. *Eur Spine J* 10(2):S96-S101.
- Anselme K. 2000. Osteoblast adhesion on biomaterials. *Biomaterials* 21(7): 667-681.
- Best SM, Porter AE, Thian ES, Huang J. 2008. Bioceramics: Past, present and for the future. *J Eur Ceramic Soc* 28(7):1319-1327.
- Bilezikian J, Raisz L, Martin J. 2008. Principles of bone biology. London, UK: Academic Press.
- Bodo M, Lilli C, Bellucci C, Carinci P, Calvitti M, Pezzetti F, Stabellini G, Bellocchio S, Balducci C, Carinci F, Baroni T. 2002. Basic fibroblast growth factor autocrine loop controls human osteosarcoma phenotyping and differentiation. *Mol Med* 8(7):393-404.
- Choi C-R, Yu H-S, Kim C-H, Lee J-H, Oh C-H, Kim H-W, Lee H-H. 2010. Bone cell responses of titanium blasted with bioactive glass particles. *J Biomater Appl* 25(2):99-117.
- Cholewa-Kowalska K, Kokoszka J, Laczka M, Niedzwiedzki L, Madej W, Osyczka AM. 2009. Gel-derived bioglass as a compound of hydroxyapatite composites. *Biomed Mater* 4(5):055007.
- Cooper LF, Masuda T, Yliheikkila PK, Felton DA. 1998. Generalizations regarding the process and phenomenon of osseointegration. Part II. In vitro studies. *Int J Oral Maxillofac Implants* 13(2):163-174.
- Foppiano S, Marshall SJ, Marshall GW, Saiz E, Tomsia AP. 2007. Bioactive glass coatings affect the behavior of osteoblast-like cells. *Acta Biomater* 3(5):765-771.

- Green LC, Wagner DA, Glogowski J, Skipper PL, Wishnok JS, Tannenbaum SR. 1982. Analysis of nitrate, nitrite, and [15N]nitrate in biological fluids. *Anal Biochem* 126(1):131–138.
- Hench LL. 1991. Bioceramics: From concept to clinic. *J Am Ceramic Soc* 74(7):1487–1510.
- Hench LL. 1998. Bioceramics. *J Am Ceramic Soc* 81(7):1705–1728.
- Hench L. 2006. The story of Bioglass®. *J Mater Sci Mater Med* 17(11):967–978.
- Holash J, Wiegand SJ, Yancopoulos GD. 1999. New model of tumor angiogenesis: Dynamic balance between vessel regression and growth mediated by angiopoietins and VEGF. *Oncogene* 18(38):5356–5362.
- Horner A, Bord S, Kelsall AW, Coleman N, Compston JE. 2001. Tie2 ligands angiopoietin-1 and angiopoietin-2 are coexpressed with vascular endothelial cell growth factor in growing human bone. *Bone* 28(1):65–71.
- Hu YC, Zhong JP. 2009. Osteostimulation of bioglass. *Chinese Med J* 122:2386–2389.
- Kasama T, Isozaki T, Odai T, Matsunawa M, Wakabayashi K, Takeuchi HT, Matsukura S, Adachi M, Tezuka M, Kobayashi K. 2007. Expression of angiopoietin-1 in osteoblasts and its inhibition by tumor necrosis factor- α and interferon- γ . *Transl Res* 149(5):265–273.
- Kieswetter K, Schwartz Z, Hummert TW, Cochran DL, Simpson J, Dean DD, Boyan BD. 1996. Surface roughness modulates the local production of growth factors and cytokines by osteoblast-like MG-63 cells. *J Biomed Mater Res* 32(1):55–63.
- Kokubo T. 2008. *Bioceramics and their clinical applications*. Abington, Cambridge, England: Woodhead Publishing Limited.
- Koller G, Cook R, Thompson I, Watson T, Di Silvio L. 2007. Surface modification of titanium implants using bioactive glasses with air abrasion technologies. *J Mater Sci Mater Med* 18(12):2291–2296.
- Landor I, Vavrik P, Sosna A, Jahoda D, Hahn H, Daniel M. 2007. Hydroxyapatite porous coating and the osteointegration of the total hip replacement. *Arch Orthop Trauma Surg* 127(2):81–89.
- Lee TM, Chang E, Wang BC, Yang CY. 1996. Characteristics of plasma-sprayed bioactive glass coatings on Ti-6Al-4V alloy: An in vitro study. *Surf Coatings Technol* 79(1–3):170–177.
- Lewinson D, Maor G, Rozen N, Rabinovich I, Stahl S, Rachmiel A. 2001. Expression of vascular antigens by bone cells during bone regeneration in a membranous bone distraction system. *Histochem Cell Biol* 116(5):381–388.
- Liekens S, De Clercq E, Neyts J. 2001. Angiogenesis: Regulators and clinical applications. *Biochem Pharmacol* 61(3):253–270.
- Livak KJ, Schmittgen TD. 2001. Analysis of relative gene expression data using real-time quantitative PCR and the 2- $^{-\Delta\Delta CT}$ method. *Methods* 25(4):402–408.
- Morris DC, Masuhara K, Takaoka K, Ono K, Anderson HC. 1992. Immunolocalization of alkaline phosphatase in osteoblasts and matrix vesicles of human fetal bone. *Bone Miner* 19(3):287–298.
- Narayan R. 2009. *Biomedical materials*. New York, USA: Springer Science+Business Media.
- O'donoghue J, Haverly D. EnBIO Ltd (Bishopstown, IE), assignee. 2008 WO2008/033867, 2008. Method of Doping Surfaces.
- O'Hare P, Meenan BJ, Burke GA, Byrne G, Dowling D, Hunt JA. 2010. Biological responses to hydroxyapatite surfaces deposited via a co-incident microblasting technique. *Biomaterials* 31(3):515–522.
- O'Neill L, O'Sullivan C, O'Hare P, Sexton L, Keady F, O'Donoghue J. 2009. Deposition of substituted apatites onto titanium surfaces using a novel blasting process. *Surf Coatings Technol* 204(4):484–488.
- Paital SR, Dahotre NB. 2009. Calcium phosphate coatings for bio-implant applications: Materials, performance factors, and methodologies. *Mater Sci Eng R Rep* 66(1–3):1–70.
- Park J. 2008. *Bioceramics: Properties, characterization, and applications*. New York, USA: Springer Science+Business Media. 364 p.
- Park B-H, Jang KY, Kim KH, Song KH, Lee SY, Yoon SJ, Kwon KS, Yoo W-H, Koh YJ, Yoon KH, et al. 2009. COMP-angiopoietin-1 ameliorates surgery-induced ischemic necrosis of the femoral head in rats. *Bone* 44(5):886–892.
- Park B-H, Yoon SJ, Jang KY, Kim M-R, Lee H-S, Kim K-B, Park H, Lee SY, Park HS, Lim ST, and others. 2010. COMP-angiopoietin-1 accelerates bone formation during distraction osteogenesis. *Bone* 46(5):1442–1448.
- Puskas BL, Menke NE, Huie P, Song Y, Ecklund K, Trindade MCD, Smith RL, Goodman SB. 2003. Expression of nitric oxide, peroxynitrite, and apoptosis in loose total hip replacements. *J Biomed Mater Res A* 66A(3):541–549.
- Rajaraman R, Rounds DE, Yen SPS, Rembaum A. 1974. A scanning electron microscope study of cell adhesion and spreading in vitro. *Exp Cell Res* 88(2):327–339.
- Santavirta S, Čeponis A, Solovieva SA, Hurri H, Jin J, Takagi M, Suda A, Konttinen YT. 1996. Periprosthetic microvasculature in loosening of total hip replacement. *Arch Orthop Trauma Surg* 115(5):286–289.
- Sargeant A, Goswami T. 2006. Hip implants: Paper V. Physiological effects. *Mater Des* 27(4):287–307.
- Sun J-Y, Yang Y-S, Zhong J, Greenspan DC. 2007. The effect of the ionic products of Bioglass® dissolution on human osteoblasts growth cycle *in vitro*. *J Tissue Eng Regen Med* 1(4):281–286.
- Tierney CM, Haugh MG, Liedl J, Mulcahy F, Hayes B, O'Brien FJ. 2009. The effects of collagen concentration and crosslink density on the biological, structural and mechanical properties of collagen-GAG scaffolds for bone tissue engineering. *J Mech Behav Biomed Mater* 2(2):202–209.
- Wang Y, Zhang S, Zeng X, Ma LL, Khor KA, Qian M. 2008. Initial attachment of osteoblastic cells onto sol-gel derived fluoridated hydroxyapatite coatings. *J Biomed Mater Res A* 84A(3):769–776.
- Xynos ID, Edgar AJ, Buttery LDK, Hench LL, Polak JM. 2000. Ionic products of bioactive glass dissolution increase proliferation of human osteoblasts and induce insulin-like growth factor II mRNA expression and protein synthesis. *Biochem Biophys Res Commun* 276(2):461–465.
- Yafan Z, Chuanzhong C, Diangang W. 2005. The current techniques for preparing bioglass coatings. *Surf Rev Lett* 12(4):505–513.
- Zinger O, Zhao G, Schwartz Z, Simpson J, Wieland M, Landolt D, Boyan B. 2005. Differential regulation of osteoblasts by substrate microstructural features. *Biomaterials* 26(14):1837–1847.